

# Nonmonotonic dependence of the absolute entropy on temperature in supercooled Stillinger-Weber silicon

Pankaj A. Apte and Arvind K. Gautam

*Department of Chemical Engineering,*

*Indian Institute of Technology Kanpur, Kanpur, U.P, India 208016*

## Abstract

Using a recently developed thermodynamic integration method, we compute the precise values of the excess Gibbs free energy ( $G^e$ ) of the high density liquid (HDL) phase with respect to the crystalline phase at different temperatures ( $T$ ) in the supercooled region of the Stillinger-Weber (SW) silicon [F. H. Stillinger and T. A. Weber, Phys. Rev. B. **32**, 5262 (1985)]. Based on the slope of  $G^e$  with respect to  $T$ , we find that the absolute entropy of the high density liquid (HDL) phase shows a nonmonotonic dependence on temperature at the liquid–liquid transition temperature of  $T_{LL} = 1060$  K. Our result is consistent with the earlier observation of a nonmonotonic dependence of the enthalpy on temperature in molecular dynamics simulations starting in the HDL phase at a temperature just above  $T_{LL}$  [S. Sastry and C. A. Angell, Nat. Mater. **2**, 739 (2003)]. Our result provides a thermodynamic route by means of which the liquid–amorphous transition occurs in SW silicon, and possibly, in real silicon.

PACS numbers: 64.70.Ja, 65.40.gd, 64.70.D-, 05.70.-a

## I. INTRODUCTION

The liquid-amorphous transition in silicon, modeled by the Stillinger-Weber (SW) potential,<sup>1</sup> has been intensely studied<sup>2–8</sup> with an aim of understanding the phase behavior of real silicon. In the initial molecular dynamics (MD) studies on SW silicon,<sup>4,5</sup> it was found that the high density liquid (HDL) phase, at a sufficiently slow cooling rate, undergoes a sudden transition to a low density amorphous phase at around 1060 K. The nature of the low density phase (i.e., whether it is a solid or a liquid) below the transition temperature was however not clear. In 2003, Sastry and Angell, through precise and careful measurements of the diffusivity in MD simulations, unequivocally showed that a low density liquid (LDL) phase exists below  $T_{LL} = 1060$  K and hence the transition should be characterized as a liquid–liquid transition.<sup>6</sup> It was also demonstrated that in constant pressure–constant enthalpy (NPH) MD simulations starting from the HDL phase at  $T > 1060$  K, the enthalpy shows a nonmonotonic dependence on temperature, ultimately leading to the formation of the LDL phase.<sup>6</sup> This was attributed to the release of latent heat during the phase transformation from the HDL phase to the LDL phase.<sup>6</sup> The purpose of this work is to perform a thermodynamic analysis pertaining to this interesting observation and reconcile all the available facts including the earlier observations of a sudden transition at 1060 K in MD cooling experiments and the uni-directionality of the transition with respect to the temperature. This last aspect refers to the finding that when the LDL phase starting at  $T < T_{LL}$  is heated slowly in MD simulations, it does not convert back to the HDL phase at  $T > T_{LL}$ , but undergoes crystallization.<sup>2,7</sup>

The primary tool that we employ is a recently developed thermodynamic integration method<sup>9–12</sup> which enables the precise measurement of the excess Gibbs free energy ( $G^e$ ) of the HDL phase with respect to the crystalline phase. The slope of  $G^e$  with respect to the temperature  $T$  yields the excess entropy  $S^e$  of the HDL phase. We then compare the changes in  $S^e$  with the changes in the absolute entropy of the crystal phase as the temperature is lowered to  $T_{LL}$  and conclude that the absolute entropy of the HDL phase  $S_{\text{HDL}}$  shows a nonmonotonic behavior with respect to the temperature at  $T_{LL}$ . In what follows, we describe the details of our computational method.

## II. SIMULATIONS OF THE HDL PHASE

To compute the excess free energy (to be described in the next section), it is important to correctly determine the average properties of the HDL phase in the supercooled region. To this end, we studied the properties of the supercooled HDL phase by performing isothermal-isobaric (NPT) Monte Carlo (MC) simulations at and above  $T_{LL} = 1060\text{K}$  and zero pressure. All of our computations were performed with a system of  $N = 512$  particles in a cubic simulation box under periodic boundary conditions. When the free energy barrier preventing crystallization of the metastable HDL phase is sufficiently high ( $T \geq 1086\text{ K}$  in the present case), there is no ambiguity in the computation of the average properties, i.e., all MC trajectories starting from different initial configurations converge to the free energy minimum relatively quickly. However when the free energy minimum corresponding to the metastable HDL phase is shallow, the probability of crossing the free energy barrier is higher and therefore proper equilibration is important to compute the correct average properties. Thus, in the temperature range of 1060–1082 K, we generated several independent MC trajectories by starting from different initial configurations. The equilibration of the trajectory in the HDL phase region was ensured by absence of a systematic decrease in the potential energy. The equilibrated trajectories at 1060 K and 1075 K are shown in Figs. 1 and 2, respectively. A systematic decrease in the potential energy per particle  $\phi'$ , as seen in these figures, indicates that the system has crossed the free energy barrier. At 1060 K, the crossing of the free energy barrier can be seen more clearly by the systematic decrease in the cumulative average of  $\phi'$  as seen in the inset of Fig. 1. The region of the trajectory corresponding to the HDL phase can thus be identified. The length of the trajectory corresponding to the HDL phase is 68 million MC steps at 1075 K (Fig. 2) and 11 million MC steps at 1060 K (Fig. 1) (Each MC step, on average, consisted of two volume change moves and  $N$  particle displacement attempts). This indicates that the free energy barrier is reduced considerably as the temperature is decreased from 1075 K to 1060 K. Further, we find that equilibrated trajectories starting from different initial configurations at a given temperature yield the same average properties, thus indicating the existence of a local equilibrium corresponding to the metastable HDL phase.

The computed average properties of the HDL phase are reported in Table 1. (The quantities reported throughout this work are expressed in units of SW potential parameters<sup>1</sup>  $\sigma$

and  $\epsilon$ , unless otherwise noted explicitly). The average densities (see Table 1) of our HDL phases at 1060 K and 1082 K are in good agreement with the previously reported values<sup>13</sup> of 0.479 and 0.482  $\sigma^{-3}$ , respectively. The computed average densities at other temperatures agree well with those found in the MD cooling experiments of Beaucage and Mousseau<sup>7</sup>.

At 1060 K, the MC trajectory upon crossing the free energy barrier, stabilizes in the LDL phase (see Fig. 1), while at higher temperatures (see Fig. 2), the MC trajectory yields a crystalline phase with defects (d-crystal phase). The LDL phase at 1060 K (see Fig. 1) has a average total energy ( $\sim -1.793\epsilon$  per particle or 375 kJ/mol) comparable to the enthalpy of the LDL phase at 1055 K found in Ref. 6 (see Fig. 1 of Ref. 6). The transition from the HDL phase to the LDL or the d-crystal phases at a given temperature involves entirely homogeneous states. This is deduced based on the observation that the following fluctuation relation<sup>14</sup> is satisfied by the MC trajectory,

$$\langle (P_v - \langle P_v \rangle)(V - \langle V \rangle) \rangle = -T, \quad (1)$$

where  $P_v$  is the instantaneous pressure in the NPT-MC simulations calculated from the virial relation<sup>15</sup> at the given instantaneous volume  $V$  and  $T$  is the externally set temperature. The symbol  $\langle \dots \rangle$  represents the average taken over the entire trajectory of the isothermal isobaric MC simulations. This fluctuation relation is derived by assuming<sup>14</sup> that the instantaneous fluctuations represents a change in state from one homogeneous phase to the other. The relation is satisfied by the entire trajectory consisting of the HDL, LDL and the defect crystal regions, as well as by the partial trajectories consisting only of the HDL phase region.

Formally, the partition function of a metastable state is defined as follows:<sup>16</sup>

$$Y(T, P, N) = \int dV \int d\mathbf{p}^N \int d\mathbf{r}^N \exp[-\beta H - \beta PV - \beta w(\mathbf{r}_1, \dots, \mathbf{r}_N)], \quad (2)$$

where  $H$  is the system Hamiltonian,  $P$  is the external pressure, and  $w = w(\mathbf{r}_1, \dots, \mathbf{r}_N)$  is an additional potential energy (to be imposed externally) that reflects back the system from the top of the free energy barrier towards the free energy minimum.<sup>16</sup> It is zero in the single phase region and takes arbitrarily large and positive values in regions beyond the free energy barrier. Thus the role of the constraining potential  $w$  is to confine the system to the metastable free energy minimum.<sup>16</sup> The probability density in isothermal isobaric ensemble is then given by,

$$\rho(\mathbf{r}^N, \mathbf{p}^N; V) = \frac{\exp(-\beta PV - \beta H - \beta w)}{Y}. \quad (3)$$

Applying the Gibbs entropy formula  $S = -k_B \langle \log \rho \rangle$ , we have

$$S = \frac{\langle H \rangle}{T} + \frac{P \langle V \rangle}{T} + \frac{\langle w \rangle}{T} + k_B \log Y. \quad (4)$$

Since the Gibbs free energy is defined as  $G = -k_B T \log Y$ , we have

$$\frac{\partial G}{\partial T} = -k_B \log Y - \frac{\langle H \rangle}{T} - \frac{P \langle V \rangle}{T} - \frac{\langle w \rangle}{T}. \quad (5)$$

Comparing Eqs. (4) and (5), we get

$$S = - \left( \frac{\partial G}{\partial T} \right)_P. \quad (6)$$

When the free energy barrier is large, the probability of reaching the top of the barrier is small and hence the quantity  $\langle w \rangle$  in Eq. (4) can be neglected. However, when the free energy barrier is small, the ensemble average  $\langle w \rangle$  cannot be neglected. In such a case, based on Eq. (4) we can conclude that  $G \neq \langle H \rangle - TS + P \langle V \rangle$ . In all of our NPT-MC simulations, we do not impose the constraint function  $w$  [see Eq. (2)], but we can still obtain the correct average properties of the HDL phase (e.g.,  $\langle \phi' \rangle$  and  $\langle \rho \rangle$ ) by ensuring equilibration of the trajectory. This is feasible due to the presence of a free energy barrier at  $T \geq 1060$  K. Nonetheless, the consideration of the reflective barrier  $w$  is, in principle, essential for defining the partition function of the metastable HDL phase.<sup>16</sup>

### III. COMPUTATION OF EXCESS GIBBS FREE ENERGY

We computed the excess Gibbs free energy difference  $G^e = G_{\text{HDL}} - G_{\text{crystal}}$  between the HDL and the crystal phases, by applying the constrained fluid  $\lambda$  integration method<sup>9</sup> in the isothermal-isobaric ensemble.<sup>10,11,17</sup> Recently, the method was found to predict the melting point of SW silicon accurately.<sup>12</sup> This is a thermodynamic integration method in which the liquid and the crystal phase are connected directly through a 3-stage reversible path. In stage 1 of the reversible path, which starts from the liquid phase, the strength of the interaction potential is reduced linearly so that the system approaches an ideal gas-like behavior. The expression for the potential energy in this stage is given by,<sup>9,10</sup>

$$\phi_1(\lambda_1) = (1 - \eta \lambda_1)U, \quad (7)$$

where  $\eta$  is a constant that determines the effective strength of the interaction potential at the end of stage 1 and  $U$  is the original inter-particle potential ( SW potential, in the present

case). The parameter  $\lambda_1$  defines the states along the path and varies from 0 to 1. As the system becomes less attractive it tends to expand. However, to maintain the reversibility of the path in stages 2 and 3, it is necessary to impose a maximum volume constraint.<sup>10</sup> The maximum constrained volume  $V_m$  is chosen such that it is slightly larger than the average volumes of the liquid and the solid phase (whichever is larger). At the same time,  $V_m$  should not affect the free energies of either of these phases.<sup>10</sup> Such a volume can be straightforwardly chosen based on the histogram of volume fluctuations for the two phases. As in an earlier work on SW silicon,<sup>12</sup> we chose  $V_m$  to correspond to a density of  $0.4\sigma^{-3}$ , i.e.,  $V_m = N/0.4$ . At the end of stage 1, we get a compressed gas phase due to the constraint on the maximum volume.<sup>10</sup> This process is depicted pictorially in Fig. 3.

In stage 2, we force the particles to form a crystalline structure by imposing an external potential in the form of Gaussian potential wells distributed on the ideal crystal lattice.<sup>9</sup> The strength of the inter-particle potential energy is held fixed during this stage. The total potential energy for stage 2 is given by<sup>9,10</sup>

$$\phi_2(\lambda_2) = (1 - \eta)U + \lambda_2 U_{ext}. \quad (8)$$

The Gaussian external potential imposed during this and the subsequent stage is given by  $U_{ext} = \sum_i \sum_k a \exp(-br_{ik}^2)$ .<sup>9</sup> Here, the index ‘i’ refers to the system particle and the index ‘k’ is a Gaussian potential well. The Gaussian well does not act on a specific particle, but exerts an influence over all the particles in its vicinity.<sup>9,10</sup> The values of the Gaussian parameters are taken to be the same as in the earlier work:<sup>12</sup>  $\eta = 0.9$ ,  $a = -1.892\epsilon$  and  $b = 8.0\sigma$ . These values are so chosen that the constrained crystalline state obtained at the end of stage 2 has almost the same energy and density as the desired crystal phase.<sup>10,17</sup>

In stage 3, the Gaussian external potential is reduced linearly to zero, while the strength of the potential energy is increased linearly to its original value.<sup>9</sup> The potential energy expression for this stage is given by<sup>9</sup>

$$\phi_3(\lambda_3) = [(1 - \eta) + \lambda_3\eta]U + (1 - \lambda_3)U_{ext}. \quad (9)$$

At the end of this stage, we get the desired crystalline phase as shown pictorially in Fig. 3.

The Gibbs free energy change for the  $i^{\text{th}}$  stage of the path can be obtained by numerical integration :

$$\Delta G_i = \int_0^1 d\lambda_i \left( \frac{\partial G}{\partial \lambda_i} \right) = \int_0^1 d\lambda_i \left\langle \frac{\partial \phi_i}{\partial \lambda_i} \right\rangle, \quad (10)$$

where  $\langle \cdots \rangle$  represents the isothermal–isobaric ensemble average at a given value of  $\lambda_i$ . The integrands for the various stages of the path at 1065 K and zero pressure are plotted in Figs. 4–6. It can be seen from these figures that the value of the integrand for the forward and the reverse paths agree well at each point. This shows that there is no hysteresis present along the path, as found earlier.<sup>12</sup>

Throughout this work, we have used the Bennett Acceptance Ratio (BAR) method,<sup>18</sup> to compute the Gibbs free energy between the adjacent states along the entire path. According to the BAR method,<sup>18</sup> the Gibbs free energy difference  $\Delta G = G_1 - G_0$  between two equilibrium states ‘0’ and ‘1’, for a given value of the constant  $C$ , is given by the following equation:<sup>18</sup>

$$\frac{\Delta G}{k_B T} = \log \frac{\sum_1 f(\beta\phi_0 - \beta\phi_1 + C)}{\sum_0 f(\beta\phi_1 - \beta\phi_0 - C)} + C - \log \frac{n_1}{n_0}, \quad (11)$$

where  $f(x) = 1/(1 + e^x)$  is the Fermi function,  $\sum_0$  and  $\sum_1$  represent the sums over Fermi functions sampled in ‘0’ and ‘1’ ensembles, respectively. The total potential energies in the two ensembles are represented by  $\phi_0$  and  $\phi_1$  in Eq. (11) and the total number of samples of the perturbation energies (or equivalently the Fermi functions) collected in MC simulations in the two ensembles are  $n_0$  and  $n_1$ . In principle, the above equation yields the correct value of  $\Delta G$  for any value of the constant  $C$ . In practice, due to the limited computational power, we cannot sample the perturbation energies in the two ensembles over all possible configurations. Thus, Bennett showed that the optimum value of  $C$ , which yields minimum error in the estimation of  $\Delta G$ , is given by<sup>18</sup>

$$\frac{\Delta G}{k_B T} = C - \log \frac{n_1}{n_0}. \quad (12)$$

Combining the above two equations, we get<sup>18</sup>

$$\sum_1 f(\beta\phi_0 - \beta\phi_1 + C) = \sum_0 f(\beta\phi_1 - \beta\phi_0 - C). \quad (13)$$

The value of the  $C$  satisfying the above equation is substituted in Eq. (12) to yield the optimal estimate of  $\Delta G$ . As mentioned in Ref. 18, the accuracy of the above method depends on the degree of overlap in the configuration space between the two ensembles. The larger the value of the two sums appearing in Eq. (13), the greater is the configuration space overlap. As prescribed by Bennett, the sum values should be much greater than unity.<sup>18</sup>

In all our computations, we ensured that the sum values are of the order of  $10^5$ – $10^6$ , by (i) performing simulations at  $\lambda_i$  values that are sufficiently close to each other (see Figs. 4–6) and

(ii) performing sufficiently long simulation runs at each of the  $\lambda_i$  values. The perturbation energies  $[(\phi_1 - \phi_0)$  or  $(\phi_0 - \phi_1)$  in Eq. (13)] required in the BAR method were collected after every MC step. At  $\lambda_1 = 0.0$  in stage 1, we used the properly equilibrated trajectories of the HDL phases, as described in the Sec. II, to collect the perturbation energy data. In stage 1, we performed upto 20 million MC steps from  $\lambda_1 = 0$  to 0.4. In the region from  $\lambda_1 = 0.4$  (stage 1) to  $\lambda_3 = 0.99$  (stage 3), we performed 0.4–0.8 million MC steps. The main source of statistical error was found to be towards the end of stage 3 due to the center of mass motion of the crystal phase as explained in detail in Ref. 12. To address this problem, we performed up to 10 million MC steps from  $\lambda_3 = 0.992$  to  $\lambda_3 = 0.999$  to collect the perturbation energy data. In the last interval of stage 3 from  $\lambda_3 = 0.999$  to 1, there is a large change in the integrand (due to center of mass motion of the crystalline phase) as seen in the inset of Fig. 6. In order to minimize the statistical error, upto 30 million MC steps were performed at  $\lambda_3 = 1$ . We ensured that the value of the sums  $\sum_0$  and  $\sum_1$  [see Eq. (13)] over the Fermi function is above  $10^5$  for all the intervals towards the end of stage 3. Further, in order to improve the accuracy three to four independent simulation runs along the entire path at all the temperatures. The statistical error for the  $i$ th stage was computed by using the formula  $\sigma_i = \sigma(\Delta G_i)/n_i^{1/2}$ , where  $\sigma(\Delta G_i)$  is the standard deviation in the  $\Delta G_i$  value and  $n_i$  is the number of statistically independent measurements. The total statistical error was computed by adding the errors for the individual stages.

#### IV. EXCESS AND ABSOLUTE ENTROPY OF THE HDL PHASE

Figure 7 shows the values of negative excess Gibbs free energy  $-G^e$  computed at various temperatures (also see Table 1) in the supercooled region at and above  $T_{LL}$ . The  $G^e$  values are comparable to those calculated by Broughton and Li<sup>2</sup> ( $\sim 25.3\epsilon$  for  $N = 512$  at 1060 K obtained by linear interpolation of the chemical potential data in Table III of Ref. 2). The excess entropy of the HDL phase  $S^e$  is equal to the slope of the curve, which we compute by the forward difference method:

$$S^e = - \frac{G_{i+1}^e - G_i^e}{T_{i+1} - T_i}, \quad (14)$$

where  $T_{i+1} > T_i$ . The values of  $S^e$  computed by above equation (for  $N = 512$ ) are reported in Table 1. The forward difference method gives the average slope (i.e. average value of  $S^e$ )



in the temperature interval  $(T_i, T_{i+1})$ . From Table 1, we find that the average value of  $S^e$  in the interval (1060 K, 1065 K) is higher by at least  $250k_B$  (after considering the error bars) compared to that in the interval (1065 K, 1070 K). Thus, as the temperature is decreased by  $\Delta T = -5$  K from 1067.5 to 1062.5 K (the mid-points of above two intervals) the change in the excess entropy is  $\Delta S^e \geq 250 k_B$ .

To estimate the change in entropy of the crystalline phase, we evaluated its constant volume heat capacity at 1060 K by using the following relation<sup>19</sup>

$$\frac{C_V}{Nk_B} = \frac{3}{2} + \frac{\langle(\delta\phi)^2\rangle}{N(k_B T)^2}, \quad (15)$$

where the quantity  $\delta\phi = \phi - \langle\phi\rangle$  is the instantaneous fluctuation in the total potential energy of the system. The average over the potential energy fluctuations was computed in the constant volume–constant temperature (NVT) MC simulations of the crystal phase and substituting this value in the above equation yields  $C_V = 3.7Nk_B$  at 1060 K. We neglect the difference between the heat capacities of the crystal phase at constant pressure and at constant volume, i.e.,  $C_P \approx C_V = 3.7Nk_B$ . Then the change in absolute entropy of the crystal phase can be estimated by the following formula,

$$\Delta S \approx C_P \log\left(\frac{T + \Delta T}{T}\right), \quad (16)$$

where we assume  $C_P$  to be constant over the temperature range of  $\Delta T$ . Using the above equation, we find that the change in the entropy  $\Delta S_{\text{crystal}}$  of the crystal phase is approximately  $-9k_B$  (for  $N = 512$ ) when the temperature is reduced from 1067.5 K to 1062.5 K ( $\Delta T = -5$  K). Since  $\Delta S^e = \Delta S_{\text{HDL}} - \Delta S_{\text{crystal}}$ , we find that  $\Delta S_{\text{HDL}} \geq 259 k_B$  for the change in temperature  $\Delta T = -5$  K from 1067.5 K to 1062.5 K. In other words, the HDL phase entropy shows a nonmonotonic dependence on temperature near 1060 K.

$$\left(\frac{\partial S_{\text{HDL}}}{\partial T}\right)_P < 0. \quad (17)$$

This is the main result of our work and we discuss its implications in the next section.

## V. SUMMARY AND CONCLUSIONS

In this work, we have computed precisely the excess Gibbs free energy  $G^e$  of the HDL phase at different temperatures by using a recently developed thermodynamic integration

method.<sup>9,10</sup> The slope of the  $G^e$  versus  $T$  curve yields the excess entropy of the HDL phase with respect to the crystal phase. Based on the change in the slope of the curve with respect to the temperature, we conclude that the absolute entropy of the HDL phase increases as the temperature is decreased to 1060 K. For a stable equilibrium phase, the entropy cannot increase as the temperature decreases. However, our result applies to the metastable HDL phase with a shallow free energy minimum. In NPT MC simulations starting from the HDL phase, we observe (see Sec. II) that system undergoes crystallization after a certain number (e.g., 11 million at 1060 K) of MC steps. Therefore the state of the isolated system containing the HDL phase and the heat bath must be considered as a constrained equilibrium state. The constraint may be imposed by means of the additional potential energy function  $w(\mathbf{r}_1, \dots, \mathbf{r}_N)$  as given in Eq. (2).<sup>16</sup>

Our findings are consistent with the nonmonotonic dependence of enthalpy on temperature observed by Sastry and Angell. In the NPH MD simulations,<sup>6</sup> the nonmonotonic loop starts in the HDL phase at a temperature just above 1060 K. As the enthalpy (or equivalently the internal energy) is reduced at zero pressure, no mechanical work is performed, and hence the lowering of internal energy must be due to the removal of heat, which implies reduction of the entropy. According to our computations, the absolute entropy of the HDL phase increases as the temperature is reduced to 1060 K. Therefore, the HDL phase at  $T > 1060$  K, upon decreasing the enthalpy, cannot transform into the HDL phase at a lower temperature. Thus the only alternative is to transform to a phase (which is intermediate between the HDL and the LDL) at a temperature equal to or greater than the starting HDL phase temperature. Note that the LDL phase has a lower enthalpy (see Fig. 1) and is expected to have a lower entropy than the HDL phase since it is structurally closer to the crystalline phase.<sup>6,21</sup> Thus, our computations show that the nonmonotonic loop starting in the HDL phase at  $T > 1060$  K,<sup>6</sup> is *induced* by the nonmonotonic dependence of the HDL phase entropy on temperature.

In the previous MD studies<sup>4,5,7</sup> it was observed that the HDL phase, at a sufficiently slow cooling rate, transforms into a low density amorphous phase at or below 1060 K. (Here by amorphous phase, we do not necessarily mean the LDL phase, but any intermediate phase between the HDL and the LDL phases). Since the process of *cooling* at zero pressure necessarily involves reduction of the entropy, the HDL phase at  $T > 1060$  K will not transform into HDL phase at 1060 K, since the latter has a higher entropy. Instead, the transforma-

tion to a low density amorphous phase (with a lower entropy) at 1060 K or below is the most natural outcome. Thus, the liquid-amorphous transition observed in the MD cooling experiments<sup>4,5,7</sup> can be explained on the basis of our result.

Recent first principles MD simulations of supercooled silicon<sup>20</sup> have found a liquid-liquid (LL) transition of a similar nature to that in the case of SW silicon. Thus we expect that SW silicon shows a qualitatively similar behavior to that of the real silicon and hence the nonmonotonic dependence of the HDL phase entropy on temperature could be the underlying cause of the LL transition in real silicon.

Finally, if one agrees that the nonmonotonic dependence of the entropy  $S_{\text{HDL}}$  on temperature  $T$  is the cause of the HDL to LDL (or amorphous) transition as argued above, then the reverse transition from the LDL to the HDL phase is feasible only if the LDL phase entropy decreases as the temperature is increased above  $T_{LL}$ , i.e., if  $S_{\text{LDL}}$  also shows a nonmonotonic dependence on  $T$ . Since the LDL phase is structurally much closer to the stable crystal phase<sup>6,21</sup> and also has a heat capacity comparable to that of the crystal,<sup>22</sup> its thermodynamic phase behavior should also be similar to the crystal phase and hence the above scenario does not seem likely. Hence the uni-directionality of the transition as observed earlier<sup>2,7</sup> can be rationalized on the basis of the expectation that  $S_{\text{LDL}}$  shows a monotonic dependence on  $T$  similar to the crystalline phase entropy.

## Acknowledgments

The authors gratefully acknowledge insightful comments by Professor B. D. Kulkarni. This work was supported by the young scientist scheme of the Department of Science and Technology, India.

---

<sup>1</sup> F. H. Stillinger and T. A. Weber, Phys. Rev. B **31**, 5262 (1985).

<sup>2</sup> J. Q. Broughton and X. P. Li, Phys. Rev. B **35**, 9120 (1987).

<sup>3</sup> W. D. Luedtke and U. Landman, Phys. Rev. B **37**, 4656 (1988).

<sup>4</sup> W. D. Luedtke and U. Landman, Phys. Rev. B **40**, 1164 (1989).

<sup>5</sup> C. A. Angell, S. Borick, and M. Grabow, J. Non-Cryst. Solids **205–207**, 463 (1996).

<sup>6</sup> S. Sastry and C. A. Angell, Nature Mater. **2**, 739 (2003).

- <sup>7</sup> P. Beaucage and N. Mousseau, J. Phys.: Condens. Matter **17**, 2269 (2005).
- <sup>8</sup> V. V. Vasisht, S. Saw, and S. Sastry, Nature Physics **7**, 549 (2011).
- <sup>9</sup> G. Grochola, J. Chem. Phys. **120**, 2122 (2004).
- <sup>10</sup> P. A. Apte and I. Kusaka, Phys. Rev. E **73**, 016704 (2006).
- <sup>11</sup> P. A. Apte and I. Kusaka, J. Chem. Phys. **124**, 184106 (2006).
- <sup>12</sup> P. A. Apte, J. Chem. Phys. **132**, 084101 (2010).
- <sup>13</sup> S. S. Ashwin, U. V. Waghmare, and S. Sastry, Phys. Rev. Lett. **92**, 175701 (2004).
- <sup>14</sup> L. D. Landau and E. M. Lifshitz, *Statistical Physics Part 1* (Pergamon Press, New York, 1980), 3rd ed.
- <sup>15</sup> M. P. Allen and D. J. Tildesley, *Computer Simulation of Liquids* (Oxford University Press, New York, 1987).
- <sup>16</sup> D. S. Corti, P. G. Debenedetti, S. Sastry, and F. H. Stillinger, Phys. Rev. E **55**, 5522 (1997).
- <sup>17</sup> P. A. Apte and I. Kusaka, J. Chem. Phys. **123**, 194503 (2005).
- <sup>18</sup> C. H. Bennett, J. Comput. Phys. **22**, 245 (1976).
- <sup>19</sup> J. L. Lebowitz, J. K. Percus, and L. Verlet, Phys. Rev. **153**, 250 (1967).
- <sup>20</sup> P. Ganesh and M. Widom, Phys. Rev. Lett. **102**, 075701 (2009).
- <sup>21</sup> V. Molinero, S. Sastry, and C. A. Angell, Phys. Rev. Lett. **97**, 075701 (2006).
- <sup>22</sup> N. Jakse, A. Pasturel, S. Sastry, and C. A. Angell, J. Chem. Phys. **130**, 247103 (2009).

TABLE I: The excess Gibbs free energy of the HDL phase with respect to the crystalline phase is listed at various temperatures for  $N = 512$  and zero pressure. The excess entropy listed in the third column is computed by forward difference method as explained in the text. The  $G^e$  data contained in this table is also plotted in Fig. 7. The fourth and the fifth columns contain the average densities and average potential energy per particle of the HDL phases. The statistical error in the computation of  $\langle\phi'\rangle$  is  $5 \times 10^{-4} \epsilon$  for  $T < 1082$  K, and  $1 \times 10^{-3} \epsilon$  for  $T \geq 1082$  K. The statistical error in the computation of  $\langle\rho\rangle$  is  $1 \times 10^{-3} \sigma^{-3}$  at all temperatures listed.

$T(\text{K})$	$G^e (\epsilon)$	$S^e/k_B$	$\langle\rho\rangle (\sigma^{-3})$	$\langle\phi'\rangle (\epsilon)$
1060	$26.09 \pm 0.02$	$1257 \pm 200$	0.478	-1.8218
1065	$25.84 \pm 0.02$	$604 \pm 200$	0.478	-1.8216
1070	$25.72 \pm 0.02$	$855 \pm 200$	0.479	-1.8195
1075	$25.55 \pm 0.02$	$683 \pm 144$	0.479	-1.8184
1082	$25.36 \pm 0.02$	$1006 \pm 252$	0.482	-1.815
1086	$25.20 \pm 0.02$	$503 \pm 252$	0.482	-1.814
1090	$25.12 \pm 0.02$	$930 \pm 100$	0.482	-1.813
1100	$24.75 \pm 0.02$	...	0.483	-1.810

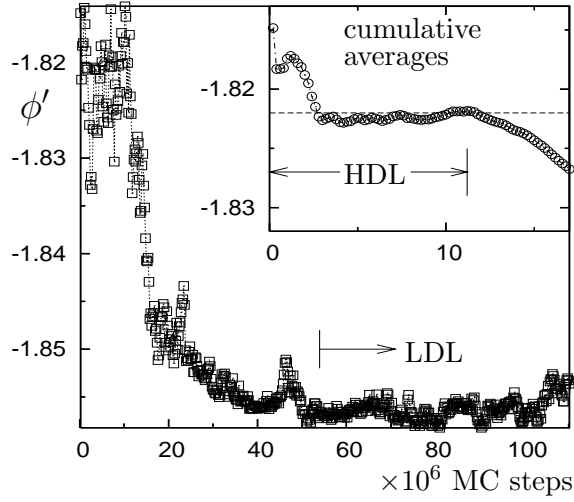


FIG. 1: The MC trajectory in terms of the potential energy per particle ( $\phi' = \phi/N$ ) at  $T = 1060$  K. The squares represent block averages taken after every 0.2 million MC steps. The LDL phase region starts (roughly) from the 52 millionth MC step onwards, as shown. The inset shows the region of the trajectory corresponding to the HDL phase. The circles in the inset are the cumulative averages obtained after the given number of MC steps on the abscissa. The dashed line in the inset is the average energy (which is the same as the cumulative average energy) of the HDL phase computed from the initial 11 million MC steps of the trajectory. A systematic and continuous decrease in the cumulative average signals the crossing of the free energy barrier.

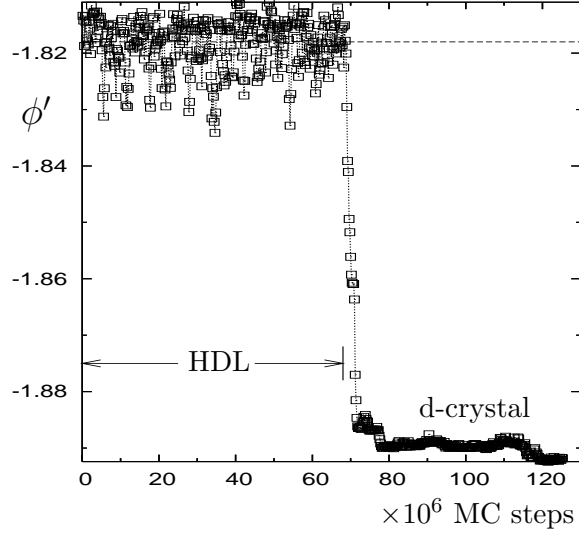


FIG. 2: The MC trajectory in terms of block averages of potential energy per particle at 1075 K. The squares are the block averages taken after every 0.2 million MC steps. The HDL phase region corresponds to the initial 68 million MC steps of the trajectory, as shown. The dashed horizontal line represents the average energy of the HDL phase. The trajectory ultimately leads to the formation of the crystalline phase with defects (d-crystal phase). The portion of the trajectory corresponding to the d-crystal phase starts (roughly) from 80 millionth MC step onwards.

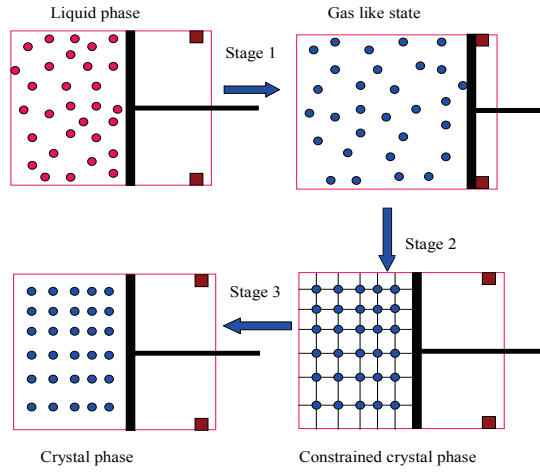


FIG. 3: Schematic diagram of the thermodynamic integration path connecting the liquid and the solid states at constant temperature and constant external pressure.<sup>9,10</sup> The stops in the piston-cylinder arrangement represent the maximum volume constraint as described in the text.



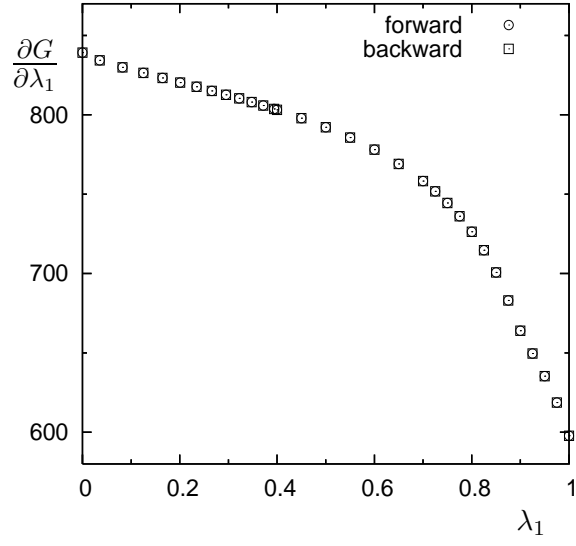


FIG. 4: The integrand (in units of the SW potential parameter  $\epsilon$ ) in Eq. (10) as a function of  $\lambda_1$  for stage 1 at 1065 K,  $P = 0$  and  $N = 512$ .

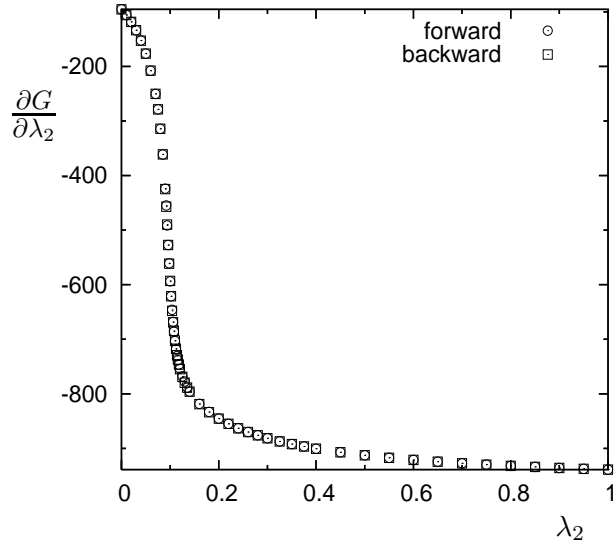


FIG. 5: The same as in Fig. 4, but for stage 2.

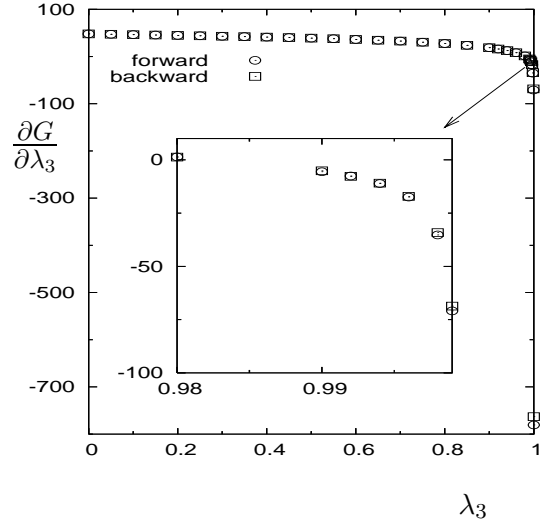


FIG. 6: The same as in Fig. 4, but for stage 3. The inset shows the region of the plot from  $\lambda_3 = 0.98$  to 0.999.

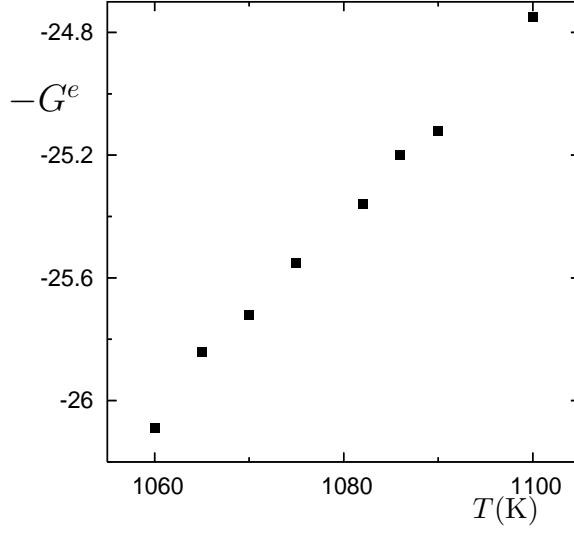


FIG. 7: The negative excess Gibbs free energy  $G^e = G_{\text{HDL}} - G_{\text{crystal}}$  (in units of  $\epsilon$ ) as a function of temperature (first and second column of Table 1) for  $P = 0$  and  $N = 512$ . The error bars (see Table 1) are smaller than the size of the symbols and hence cannot be seen. The slope of the curve yields the excess entropy  $S^e$  of the HDL phase with respect to the crystalline phase. A large increase in the slope is seen as the temperature is lowered to 1060 K, indicating an increase in the excess and the absolute entropy of the HDL phase as discussed in the text.